EXPERIMENTAL AND NUMERICAL RESEARCH INTO LOCAL CONTACT EFFECTS IN MASONRY

A.T. Vermeltfoort[1]
[1] Assoc. Professor, Department of the Build Environment, Eindhoven University of Technology, Eindhoven, The Netherlands, a.t.vermeltfoort@tue.nl

ABSTRACT
In load-bearing walls made of calcium silicate elements two types of joints can be recognized: joints between two elements and joints between wall and floor. Ideally, the mortar joints are completely filled and consequently stresses are transmitted uniformly through masonry. However, sometimes only the joint-edges are filled, like in shell bedded masonry. This causes irregularities in the stress distribution. Another situation with local contact effects where stresses are not uniformly distributed is the wall-floor connection when centering strips are applied. These strips are intended to concentrate the loads from the floor and to improve the floor wall interaction. To study the effects of such local contacts on the load bearing capacity of walls, 85 experiments and numerical simulations of these experiments were performed with parameters like the joint filling ratio and the width and position of the bearing strip. Relationships between the load bearing capacity and the main parameters were established.

KEYWORDS: bearing strip, local contact, face shell bedded masonry, splitting strength

INTRODUCTION
Well designed masonry walls are capable to carry loads from floors and walls above. However, local contact effects that occur in the relative small area around joints may reduce the bearing capacity. In this paper we focus on the effects of a) partly filled joints (PFJ) and b) centring strips (CSt) in the wall-floor joint on the load bearing capacity of masonry walls.

Centering strips are used when floors are relatively slender, i.e. floors with a large span-thickness ratio. Then it may be necessary to increase the rotation capacity of the floor-wall connections. This can be done by placing strips, so called centering strips, narrower than the thickness of the wall on top of the wall. In this way, the load from the floor is concentrated and more freedom of rotation is obtained. For a large rotation capacity the width of the strip must be small, however, a small width causes higher splitting stresses in the wall. To date, no explicit rules or design guidelines are available for the design and control of centering strip connections. Figure 1 shows the different deformation schemes for rigid and free-rotating connections in a floor wall system.

Width, thickness and type of material of the strip play an important role in the deformation. A flexible material with relatively much deformation at small loads is preferred because the effect of eccentric loading will be smaller compared to the use of a stiff material. Therefore, often rubber is used for centering strips.

The ideal position of the strip is in the centre of the wall. In practice, the strips are sometimes positioned out of centre. This may affect the load bearing capacity.

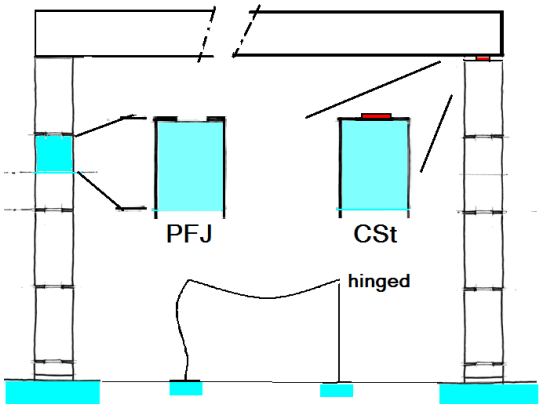

Figure 1: Wall, four layers of 600 mm high elements. Details of PFjoints and centre strip. Floor deformation, with and without centering strip, i.e. rigid or hinged connection.

Partly filled joints should be avoided. However, often joints are only partly filled due to laziness or to save material. Then, instead of using the appropriate tools to fill the joint completely, a trowel is used to apply some mortar only at the edge of the wall. The main parameter in this case is the total width of the two strips of mortar, (g).

To study the behaviour of the joint and the material relatively close to the joint, only a representative part of a wall is needed for experiments. This wall-part will contain at least one joint and a certain amount of calcium silicate. In a wall built of elements only a few joints are present so they will not affect each other, Figure 1. It is assumed that stresses are uniformly distributed at mid height of an element. Therefore, the chosen model is bordered by a line through the centre of the joint and one at a sufficient distance from the joint, Figure 1.

For comparison of results, the specimens overall strength (*f'w*) is used. Therefore, the ultimate load is divided by the cross section of the specimen, Equation (1):

$$f'w = \frac{Fult}{A} \tag{1}$$

with:

F_{ult} = maximum force observed in the experiment

A = loaded area of the specimen

MATERIALS USED

Since the mid 1980s the use of CASIELs in medium sized buildings has become popular. The Calcium-Silicate industry has developed a complete program of building load-bearing walls, from design to finished walls, Berkers 1995 [1], Vermeltfoort and Ng'andu 2007 [2].

Compressive strength is one of the main properties used in the design of load bearing masonry. Other properties are related to it, like tensile strength. For quality control purposes, the compressive strength is determined from crushing tests on cubes or prisms cut out of elements at predetermined positions, EN 771-2:2003 [3]. The specimens were made of CS20 elements, a commonly used quality with a unit compressive strength (f_b) of 20 MPa and a tensile splitting

strength of 2 MPa. Walls made of this quality of units will have a characteristic compressive strength (f_k) of 10.2 MPa, according to EC6 [4]:

$$f_k = K \cdot f_b^{0.85} \quad (2)$$

With K = 0.8. The Young's modulus of CS20 masonry is between 8000 and 10000 MPa, Vermeltfoort [2].
Based on experience, the moisture content of the test-specimens was estimated to be between it 2% en 3% in the given conditions.
The mortar must be of a certain minimal quality but according to Equation (2) mortar strength has little or no effect on compressive wall strength.

Centering strips were made from Styrene butadiene rubber (SBR). Some indicative material properties are: SBR is moderate weather resistant and not oil resistant. Temperature boundaries range from -10^o to 70^o C. Tensile strength is 2.5 MPa, Strain at fracture 150%. Volumetric mass 1.4 g/cm3. Shore hardness 70^o +/-5. Maximum compressive strength 5.0 MPa. The manufacturer declared a Young's modulus varying from 10 to 100 MPa; depending on the maximum occurring strain. However, when a piece of rubber is confined between stiffer materials, its behaviour will be much stiffer than in a "free" compressive test.

LITERATURE

The behaviour of face shell bedded hollow block masonry was studied by Maurenbrecher [5]. The hollow concrete blocks with a relatively large diaphragm differed from masonry made from solid calcium silicate elements, but the image of the force transfer found in the blocks may be useful. Also Hendry [6] and Drysdale [7] discuss the problems around of partly filled joints in masonry made of hollow blocks but general design rules are not given. Literature, [5], [6] and [7] shows that in face shell bedded masonry the stress distribution near the so called webs is disturbed because of the partly filled joint. For parts outside the ambit of the webs the stress distribution remains uniform. In masonry made of solid blocks, the disturbance of stresses occurs over the full volume.

In paragraph 3.6.1.3. from EN 1996-1-1 (EC6) [4] titled: "Characteristic compressive strength of Shell bedded masonry" rules are given to establish the compressive strength (f_k) of shell bedded masonry, and a constant K is used (Equation 2). For walls with thickness t and width of mortar joint g, rule 4 reads: "K is taken from paragraph 3.6.1.2 when g/t=1 (completely filled joint) or K is taken as half of those when g/t=0.4, with intermediate values obtained by linear interpolation". For thick walls with narrow mortar strips, i.e. g/t<0.4 no criterion is given in EC6.

At floor-wall connections with centering strips a relatively large force has to be transmitted via a relatively small contact surface which results in high stresses in the contact area.
At the connection of structural elements often similar situations occur, for example for beams or lintels resting on walls. Studies, e.g. Page [8], show that the material just below the connection is in a 3D compressive stress state. Further away, stresses fade out in the supporting wall. Consequently, at some distance from the support, the vertical compressive load causes tension in both horizontal directions, which, certainly in thickness direction, may lead to splitting of the wall. Of course, the magnitude of the stresses depends on the size of the contact area and its position on the wall, and the thickness of the wall. This kind of stress conditions also occur below centre strips and at openings due to partly filling of joints.'

TEST SET UP

As discussed earlier, only a relatively small part of a wall was studied. Therefore, blocks were cut form elements with a size big enough to allow for an area around the problem zone to spread the stresses resulting in a more or less uniform stress distribution at the opposite edge.
The cut bottom surface was positioned on the bottom loading plate. The top edge simulated the joint (PFJ) or the wall-floor connection (CST). Table 1 shows the types of tests and the number of specimens used.

Dimensions of specimens were as follows (Table 1):
- Specimen width was equal to wall thickness; i.e. thickness of elements. For PFJ tests this was 300mm, for CST tests this was 200 mm or 214 mm.
- Specimen thickness for PFJ tests was 70 mm, for CST test it was 100 mm. In later tests it was 200 mm due to the observed bulging effects caused by rubber strip. In PFJ tests thickness showed to be less critical due to the smaller difference in Poisson's ratio between mortar and calcium silicate compared to Rubber and calcium silicate.
- The height-width ratio of all specimens was large enough to obtain a uniform stress distribution at the full loaded bottom surface. Load introduction on the top of the specimen introduced an uneven stress distribution which faded out to the bottom as indicated by linear elastic numerical simulations, Figure 3 shows a contour-plot of the horizontal stresses in a specimen loaded via a 70 mm wide strip.

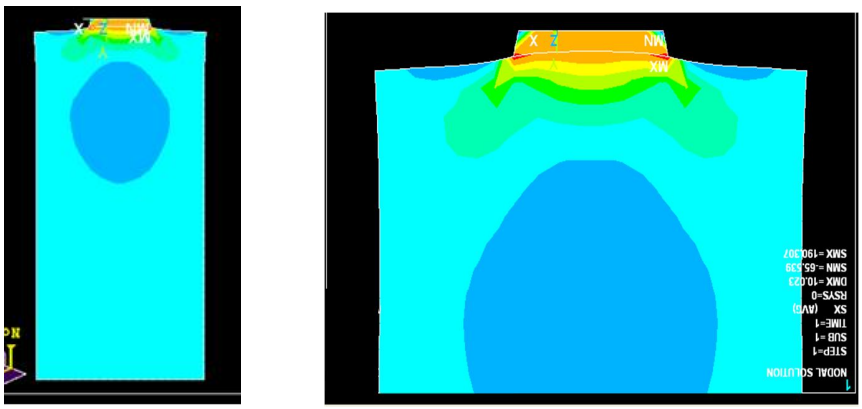

Figure 2 Horizontal stresses in a prism loaded centrically via a 70 mm wide strip, left whole specimen, right zoomed in. Printed upside down for ease of comparison with experiments.

Figure 3 shows the different load introduction principles used. The width of the joint (v = g/2) of the face shell bedded tests (Figure 2A) was varied. In the centre strip tests (CSt) the width of the centre strip was varied (CSw, Figure 2B), or the 40 mm wide strip was positioned eccentrically (CSe, Figure 2C) or the load was positioned eccentrically on a 70 mm wide, centrically placed strip (CSp, Figure 2D). Line CL in Figure 2 represents the centre line of the loading machine. The bottom of the specimens was a cut surface, the top, with mortar or centre strip, was as it would have been in real situation.

Two CSTw tests were done with 4 mm wide wooden "strips". These tests resembled the Brazilian splitting tests [9], [10]. At edges of a centering strip or mortar, situations comparable with the situation in a splitting test occur, so load bearing capacity may be related to splitting strength.

Table 1 Types of tests and number of specimens

	Dimension mm3	type of test and number of tests	total #
CSw	100 x 214 x 400	strip width in mm 4, 25, 50, 75, 100, 214; each test in threefold	18
CSe	200 x 200 x 400	position of 40 mm wide strip, eccentricity 0, 10, 20, 30, 40, 50, 60, 70 mm	11
CSp	200 x 200 x 400	position of load on a 70 mm wide strip: 0, 5, 10, 15, 20 mm; each test twice	10
PFJ	300 x 300 x 70	joint width (v = g/2) in mm 20, 40, 60, 77, 120, 150 each test was performed 7 or 8 times	46

PFJ: Face Shell Bedded; CSt : Centering Strip Test.

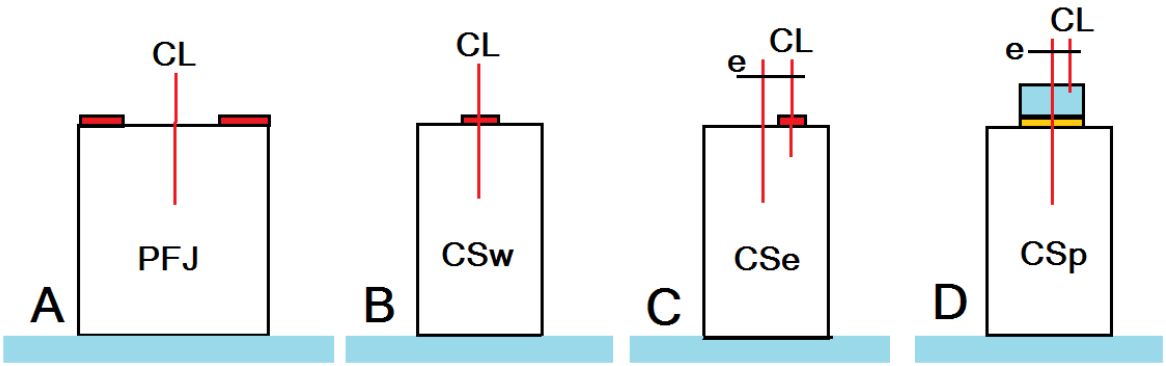

Figure 3 Load introduction principles. CL = centre line of loading

Strips were cut from larger 5 mm thick, 80 mm wide rubber strips in the appropriate length and width. When strips had to be wider than 80 mm two strips of equal width were positioned besides each other. The centering strips were put on top of the specimen in the appropriate position. In this way, the building practice situation was simulated. The block-strip combination was positioned in the machine in such a way that the centre line of the machine coincided with the centre of the strip. This was done to minimize the chance on rotation of the top-load platen. The specimens were placed on the load platen of the testing machine with their cut surface. The machined surface was on top.

The CSp-specimens with load introduction type D were loaded via a steel block on the 70 mm wide centre strip. On this steel block, a brass strip of 4 x 4 mm^2 was placed to concentrate the load. The position of this brass strip was varied in steps of 5 mm between 0 mm and 20 mm (Table 1). With these eccentricities the effect of the rotation of the floor was simulated; that means, the floor would then rest more to the edge of the wall. Similar with the other tests, the specimen was positioned out of centre and the bras strip in the centre of the testing machine.

Specimens with partly filled joints (PFJ) were positioned in the centre of the testing machine and needed no further preparation. Earlier the joint mortar was applied in strips. The width of the strips was the studied parameter in this series of tests. Mean mortar compressive strength was 18.4 MPa (STDev. 0.77 MPa). A double layer of greased PE foil was positioned between the mortar and the load platen to allow for free lateral movement.

Material from three deliveries was used, material A for PFJ, material B for strip width testing and material C for strip position and position of load on strip tests. Tensile splitting strength was 1.90 MPa for material A and 2.06 MPa for material B.

SIMULATION PFJ

To develop an analytical model, the force transfer in the PFJ specimen is compared to that in a deep beam. In a beam with sufficient height in relation to its span an arch shaped area will develop, Figure 4. This area is in compression while the bottom edge, connecting both supports is under tension and acts as a tie. If it is assumed that deep beam theory is applicable, then bending stress is proportional to the applied uniformly distributed load and consequently failure load will be proportional to joint width.

The magnitude of the stresses depends on the height of the arch which in its turn depends on the distance of the filled joint parts i.e. the span. Deep beam theories suggest an arch height (h) of approximately 0.6 times span length (L) which is a little more than the distance between both joint edges, Figure 3.

The scheme in Figure 4 also shows that due to arch action, vertical stresses at the inner edge of the supports will be larger than those at the outer edge, because the arch is wider than the support. Peak stresses near the mortar edge may be expected, also due to singularity in point A, Figure 4.

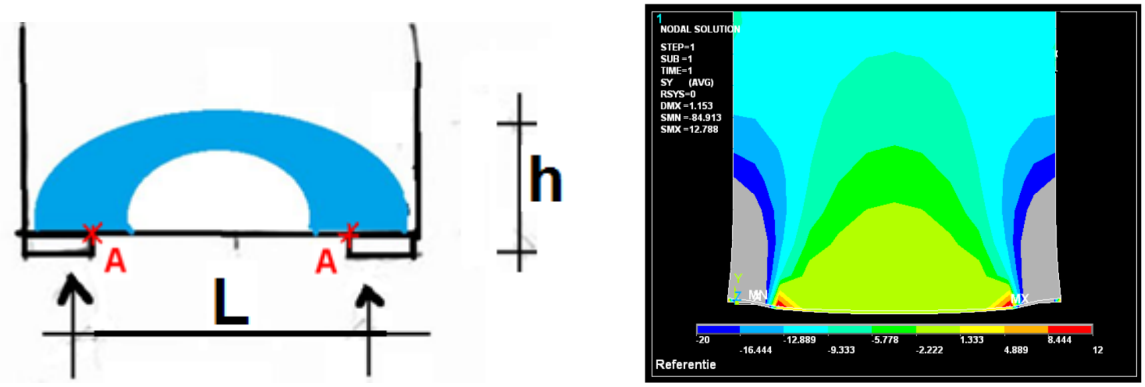

Figure 4 Scheme compressive stresses in the shape of an arch, stress contour.

A numerical model for the partly filled joint situation was developed, using parameters. In this way, joint width could easily be changed and all related dimensions were automatically adapted. The following material properties were applied: E_{CaSi} = 9000 MPa, E_{mortar} = 7000MPa and $E_{interface}$ = 9000 Mpa. Element type Plane 82 was used with an element size of 30 mm.

Figure 4 shows that (tensile) stresses developed at the bottom between the two joint edges. This was already seen in the analytical model. Close to the mortar compressive stresses develop and in perpendicular direction tensile stresses. Close to the inner vertical edge of the joint (point A in Figure 4A) peak stresses occurred. See also Figure 4B. The arch-shape is clearly visible in the contour plots.

Horizontal stress distribution is similar to that found in deep beams [11]. In Figure 5 stress distribution over height is plotted for different values of joint width (v = g/2). Figure 7 shows that the tensile stress (σ) in the bottom edge is proportional to joint width (v) according to:

$$\sigma = -0.089*v + 17.61 \quad [MPa] \tag{3}$$

Consequently, failure load will be reversed proportional to joint width and proportional to tensile strength of the calcium silicate elements used.

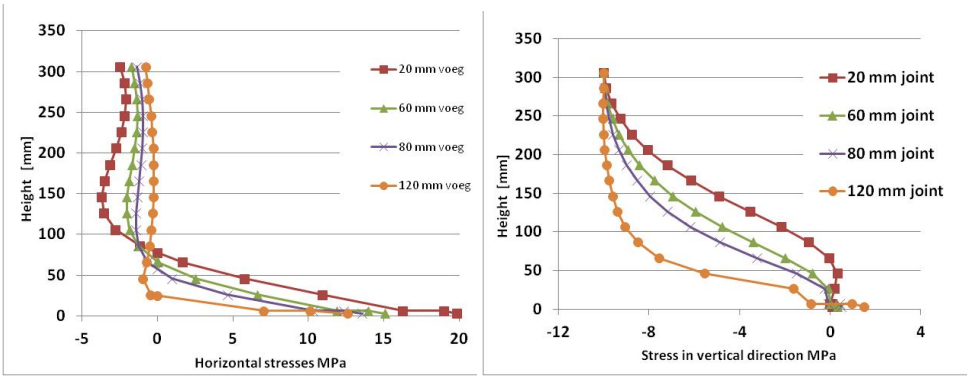

Figure 5 A Horizontal (left) and B vertical stresses in the vertical mid section.

In Figure 5B the stress in vertical direction, on a vertical line in the centre of the specimen, is plotted versus height for various joints widths (v = g/2). These vertical stresses are equal to the applied stress of 10 MPa at the top edge and relatively small at the bottom because of the open joint. Depending on the amount of joint filling, stresses remain longer equal to the applied stress, Figure 5B.

Figure 6 shows vertical stresses at the bottom edge for joint widths of 60 mm and 120 mm respectively. Near the mortar edges the expected peak stresses, as discussed earlier, really occur.

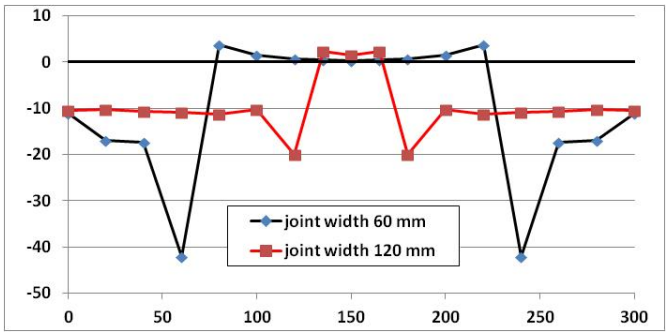

Figure 6 Vertical stresses in and near the supports (joint) versus specimen's width for joint widths 60 and 120 mm. Peak stresses near the edge of the joint mortar, 10 MPa applied load. Relatively small vertical tensile stresses in the area between both joints.

Figure 7A shows the decrease of inner lever arm length with increasing joint width (i.e. decreasing span length) as expected. Tensile bending stresses at a vertical mid span section decrease with increasing joint width as shown in Figure 7B. These horizontal stresses at the bottom edge are reversed proportional with joint width.

EXPERIMENTAL RESULTS

The course of all tests was similar. At a load of 13 kN the closing of the play of the system was recognized. This was possible because the change in distance of the bottom and top load platen was measured.

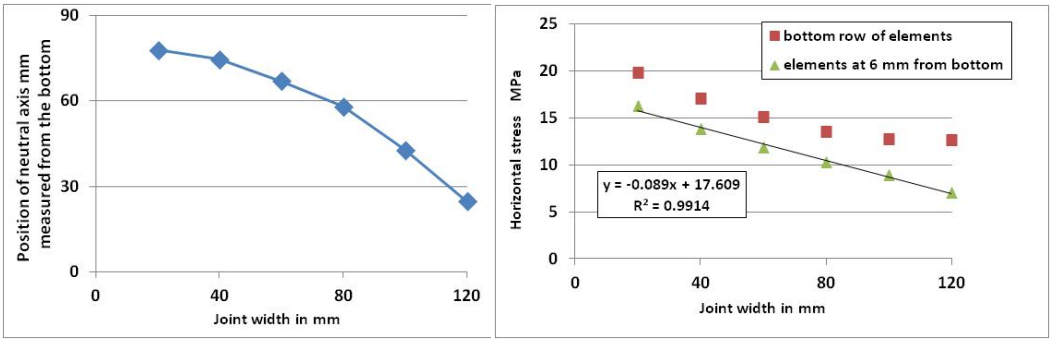

Figure 7 A. Decrease of the height of the neutral axis with increasing joint width and B stresses in horizontal direction in the bottom edge versus joint width.

In the 100 mm thick CSTw-tests, at a load of approximately 65% of the ultimate load, irregularities in the load deformation graph were observed. This was caused by spalling of the sides of the specimen, directly below the centering strip due to the bulging out of this strip. (Poisson's effect). Based on this observation, the other CST specimens were made 200 mm thick.

In the PFJ tests, a fast drop of the load (approximately at 50% of Fult) is observed, whereupon the earlier course was resumed, Figure 9A. This drop was caused by some vertical cracking, which stopped due to the confining effect of the load platen. The greased polyethyleen sheets used still had some fiction resistance.

Main characteristic of the failure of all specimens was the development of a vertical crack, either in the centre of the centering strip (Figure 8B) or at the edge of the strip (Figure 8A) or the mortar joint edge in PFJ tests. In some tests, the load dropped rapidly after cracking started, (brittle behaviour) in other tests this process was more steadily. After cracking of the PFJ specimens, the confining effect at the mortar-load introduction areas may have contributed to the load bearing capacity. Greased polyethylene sheets were used to reduce this effect but some confinement still may have been possible. Finally, when the FSJ-specimen failed, a vertical crack developed, splitting the block in two halves, Figure 8.

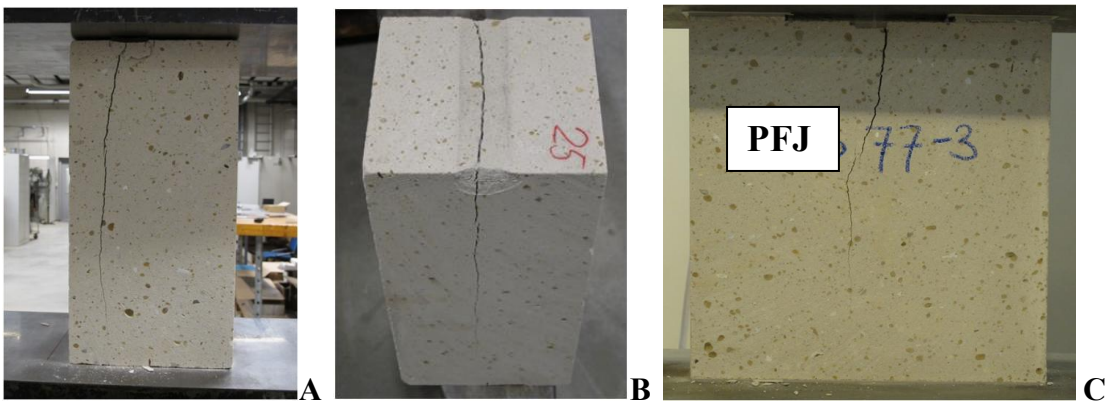

A **B** **C**

Figure 8 Splitting of specimens and traces of the centre strip after testing.

When a symmetric specimen is loaded symmetrically its deformed shape will be symmetric as well. Bending will not occur. However, when loaded eccentrically the top of the specimen will not only move in vertical but also in horizontal direction. When in a test lateral deformation is partly prevented horizontal reaction forces will develop. For practical reasons no measurements

were taken to prevent the development of horizontal forces. It is assumed that these forces would be relatively small due to the deformation properties of the centering strips.

PFJ experimental results

The overall strength, f'_w, was established according to Equation (1). The results of 46 tests on specimens with partly filled joints are plotted versus the width of the unfilled part (uf) of the joint (uf = 300 - 2*v) in Figure 9B. The compressive stress in the joint (f'_j) is given as well.

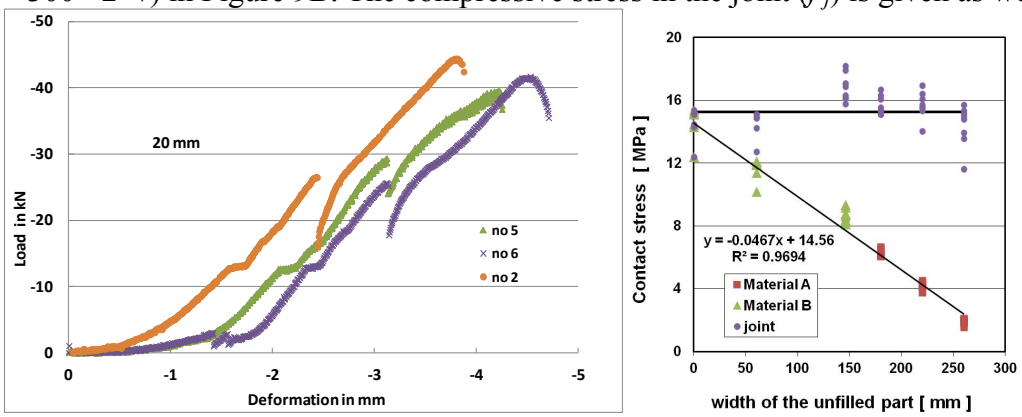

Figure 9 A) Example of Load-displacement diagram of centre strip tests B) Contact stress plotted against width of the unfilled part of the joint. The compressive stress in the joint is indicated with dots. The mean value is 15.22 MPa (C.o.V. = 6.7%).

Figure 9B shows that in partly filled joint specimens the bottom stress (f'_w), is linearly related to uf; i.e. to joint width (v = g/2) as well. The best fit linear relationship in Figure 9 had a $R^2 = 0.97$. From this it can be concluded that in all FSB-specimens failure occurs at approximately the same stress (f'_j) in the contact surface between mortar and calcium silicate while $f'_b = f'_j$*(t-uf)/t with $f'_c \sim 14.56$ Mpa and t = 300 mm. The mean value of the 46 tests for f'_j was 15.22 MPa.

According to EC6 it may be assumed that when the joint is filled for four tenth (g/t = 0.4) the strength is half of the strength of masonry with completely filled joints. According to the found relationship, strength is not half but four tenth of the strength of masonry with completely filled joints. That means EC6 overestimates the strength with a factor 1.25.

CSt experimental results

The contact stress (f'_w) of the three series of tests on specimens with centering strips is plotted versus a) the width of the strip, b) the position of the strip and c) the position of the load on the strip in Figures 10A, 10B and 10C respectively

The results of the tests with 4 mm wide wooden strips were in line with the other tests with wider strips and as expected, compared to splitting tests results (Brazilian test [9], [10]). However, the specimen was only loaded from one side.
When the trend shown in Figure 10A is extrapolated to a strip width equal to block width (= wall thickness) an f'_w of 14 MPa is expected. In the experiments a mean value for the failure load of a block was 17 MPa, a difference of approximately 30%, however, blocks were tested without rubber interface. Expanding rubber decreases load bearing capacity.

The contact stress appears to be proportional to strip width even with narrow strips. This relationship is similar to the one found with the PFJ tests.

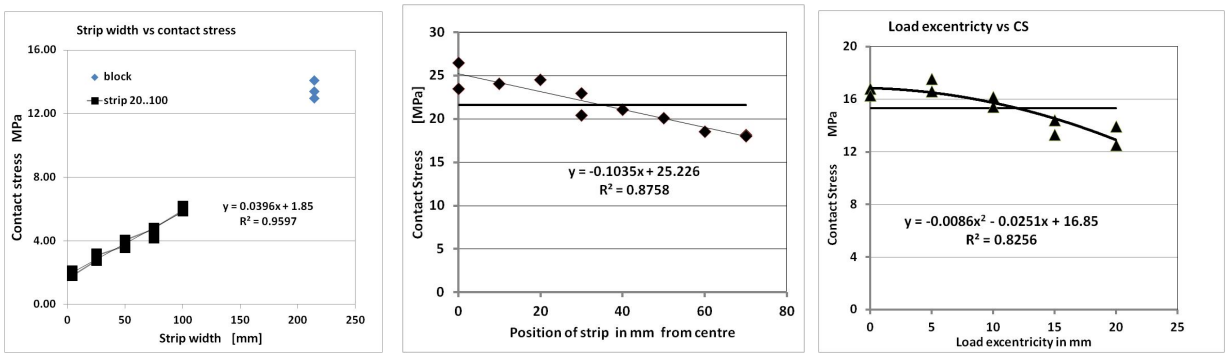

left: variable strip width, middle 40 mm wide strip, right, 70 mm wide strip.

Figure 10 Effect of A) strip width, B) strip position and C) position of load on ultimate contact stress.

Eccentricity of the load negatively affects the overall strength (f'_w) both in the tests with eccentric positioned strips (CSe) as in the tests with eccentric positioned load (CSp) as shown in Figure 10B and 10C.

Both in the CSe (eccentric strip position) as in the CSp (eccentric load position) the eccentricity of the axial load causes bending in the specimen. In the CSe tests this effect faded out over a shorter distance than in the CSp tests resulting in linear trend in Figure 10B. In the CSp tests, the stresses directly below the strip are relatively higher compared to the stresses below an eccentric positioned strip that is loaded more or less uniformly.

The maximum stress increases quadratic with increasing eccentricity while for larger eccentricity of the load the contact area becomes smaller, as if the interface "cracks". Therefore a parabolic trend line is drawn in Figure 10C.

CONCLUSIONS

The following relationships between mean overall strength (f'_w; in MPa) and (a) unfilled part of the joint (uf); (b) strip width (sw), (c) strip eccentricity (es) and (d) eccentricity of load on strip (le), with uf, sw, es and le in mm, were found:

$f'_w = -0.0467\ uf + 14.56$ (R2 = 0.97; 46 tests; t = 300 mm) (4)

$f'_w = 0.0396\ sw + 1.85$ (R2 = 0.96; 18 tests; t = 214 mm) (5)

$f'_w = -0.1035\ es + 25.226$ (R2 = 0.88; 11 tests; t = 200 mm) (6)

$f'_w = -0.0086\ le^2 - 0.0251\ le + 16.85$ (R2 = 0.82; 10 tests; t = 200 mm) (7)

These relationships may depend on dimensions and material used.

Equation (4) shows that compressive strength for masonry with incompletely filled joints depends on joint width (uf = t - 2*v) and that ultimate stress in the joint (f'_j) is almost independent from joint width; Figure 11. The result from Equation (4) differs from the result that would have been obtained using EC6 [4]. EC6 overestimates the strength (f'_k) with a linear decreasing factor from 1.25 for g/t = 0.4 to 1.00 for g/t = 1 compared to the specimen's overall strength (f'_w).

Equation (5) shows that the compressive strength (f'_w) increases with wider strips (sw), similar to the effect of larger joint filling (uf = t - 2*v) in PFJ tests.
Equation (6) and (7) show that eccentricity of loading has a negative effect on compressive strength.

Arching action in PFJ specimens, known from literature is numerically confirmed. The height of the arch varied with the distance between the supports (i.e. the unfilled parts of the joint).

In the numerical studies, places were recognized with high peak stresses; i.e. in the middle between the two joint-parts and at the joint edges of the specimens with incompletely filled joints and at the edge of centering strips. Subsequent research could be aimed at finding at which position the tensile stresses are most critical in relation with the formation of cracks.

For the tests discussed in this paper relatively small specimens were used with boundary conditions that were different from reality, while lateral deformation was not completely free. Therefore, further research is needed to study the effects of the parameters on the behavior of a complete wall, in which buckling effects may become more critical as well.

Subsequent research also may be aimed at:
- the effects of variation in joint width over the length of a wall while the mortar strip width may vary because of practical reasons
- the effects of variation in properties of materials used, like mortar, calcium silicate unit or centering strip material strength and Young's modulus and perhaps other properties.
In experiments a block length larger than 200 mm should be considered to obtain results representative for long walls.

REFERENCES.

1. Berkers, W.J.G., 1995, Building with calcium silicate elements, Proc. 4th Int. Mas. Conf., London, Vol 1, (7) pp. 176-177
2. Vermeltfoort, A.T. & Ng'Andu, B.M. (2007). Design considerations and the use of CASIELs in medium rise buildings. Proc. of the 3th Int. Conf. on Structural Engineering, Mechanics and Computation (SEMC 2007), Cape Town, South Africa (pp. 1-6).
3. /…../, 2003, NEN-EN 771-2:2003, Specification for masonry units - Part 2: Calcium silicate masonry units, Nederlands Normalisatie Instituut, Delft.
4. /…/, EN 1996-1-1, 2005, Eurocode 6. Design of masonry structures. General rules for reinforced and unreinforced masonry structures. European com. for standardization, Brussels.
5. Maurenbrecher, 1986, Compressive strength of hollow concrete blockwork, Proc. 4th Can. Mas. Symp. pp. 997-1009.
6. Hendry, A.W., Sinha, B.P. and Davies, S.R., 1987, Load Bearing Brickwork Design, 2nd edition, Ellis Horwood Ltd., ISBN 0 745 0183
7. Drysdale, R.G., Hamid, A.A. and Baker, L.R., 1993, Masonry structures, behaviour and design, Prentice Hall, Englewood Cliffs, New Jersey.
8. Page A.W., 1988, Finite Element Model for Masonry Subjected to Concentrated Loads, Journal of Structural Engineering, Vol. 114, No. 8, August 1988, pp. 1761-1784.
9. Mier, J.G.M. van, 1997, Fracture processes of concrete, CRC Press, Boca Raton, U.S.A.
10. Indirect tensile test on concrete cylinders. Preliminary investigations. Rapport BI-55-19. I.B.C.-T.N.O. via http://heronjournal.nl/4-3/1.pdf